

Multifrequency behaviour of the anomalous events of PSR J0922+0638

G. Shaifullah,^{1,2,3}★ C. Tiburzi,^{2,3} S. Osłowski,⁴ J. P. W. Verbiest,^{2,3} A. Szary,^{1,5}
 J. Künsemöller,² A. Horneffer,³ J. Anderson,⁶ M. Kramer,^{3,7} D. J. Schwarz,² G. Mann,⁸
 M. Steinmetz,⁸ and C. Vocks⁸

¹ASTRON, The Netherlands Institute for Radio Astronomy, Postbus 2, NL-7900 AA Dwingeloo, the Netherlands

²Fakultät für Physik, Universität Bielefeld, Postfach 100131, D-33501 Bielefeld, Germany

³Max-Planck-Institut für Radioastronomie, Auf dem Hügel 69, D-53121 Bonn, Germany

⁴Centre for Astrophysics & Supercomputing, Swinburne University of Technology, PO Box 218, H11, Hawthorn, VIC 3122, Australia

⁵Janusz Gil Institute of Astronomy, University of Zielona Góra, Lubuska 2, PL-65-265 Zielona Góra, Poland

⁶Deutsches GeoForschungsZentrum, Telegrafenberg, D-14473 Potsdam, Germany

⁷Jodrell Bank Centre for Astrophysics, University of Manchester, M13 9PL Manchester, UK

⁸Leibniz-Institut für Astrophysik Potsdam (AIP), An der Sternwarte 16, D-14482 Potsdam, Germany

Accepted 2018 March 22. Received 2018 March 22; in original form 2018 February 16

ABSTRACT

PSR J0922+0638 (B0919+06) shows unexplained anomalous variations in the on-pulse phase, where the pulse appears to episodically move to an earlier longitude for a few tens of rotations before reverting to the usual phase for approximately several hundred to more than a thousand rotations. These events, where the pulse moves in phase by up to 5° , have been previously detected in observations from ~ 300 to 2000 MHz. We present simultaneous observations from the Effelsberg 100-m radio telescope at 1350 MHz and the Bornim (Potsdam) station of the LOw Frequency ARray at 150 MHz. Our observations present the first evidence for an absence of the anomalous phase-shifting behaviour at 150 MHz. Instead, the observed intensity at the usual pulse-phase typically decreases, often showing a pseudo-nulling feature corresponding to the times when phase shifts are observed at 1350 MHz. The presence of weak emission at the usual pulse-phase supports the theory that these shifts may result from processes similar to the ‘profile-absorption’ expected to operate for PSR J0814+7429 (B0809+74). A possible mechanism for this could be intrinsic variations of the emission within the pulsar’s beam combined with absorption by expanding shells of electrons in the line of sight.

Key words: radiation mechanisms: non-thermal – pulsars: general – pulsars: individual: J0922+0638, B0919+06.

1 INTRODUCTION

Pulsars are rapidly rotating magnetized neutron stars which show extreme rotational stability on time-scales of decades (Petit & Tavella 1996; Verbiest et al. 2009). However, almost all classical (or ‘slow’) pulsars and a few millisecond pulsars (MSPs) exhibit significant and typically small-scale deviations from their stable rotational behaviour. These may include stochastic, wideband, pulse-to-pulse variations (Cordes 1993; Osłowski et al. 2011) due to unknown processes or, variations on short time-scales like glitches (Radhakrishnan & Manchester 1969; Reichley & Downs 1969; McKee et al. 2016), profile mode changes (Backer 1970c), and nulling (Backer 1970b). Apart from these, pulsars also display well-known phenomena such as drifting subpulses (Backer 1970a), polarization modes

(Gangadhara 1997; van Straten & Tiburzi 2017), microstructure (Johnston et al. 2001), and profile ‘absorption’ where part of the profile is obscured (see e.g. Rankin, Ramachandran & Suleymanova 2006b). A recent addition to these phenomena are ‘emission shifts’ where the emission briefly shifts to an earlier longitude, first identified by Rankin, Rodriguez & Wright (2006a) for PSRs J1901+0716 (B1859+07) and J0922+0638 (B0919+06).

PSR J0922+0638 is a bright, isolated pulsar which has a spin period of ~ 0.43 s. It is located about $1.1_{-0.1}^{+0.2}$ kpc away (Chatterjee et al. 2001) and has associated dispersion and Faraday rotation measures of $27.2986(5)$ pc cm⁻³ and $29.2(3)$ rad m⁻² (DM and RM, values taken from Johnston et al. 2005; Stovall et al. 2015, respectively). Due to its relative brightness PSR J0922+0638 has been observed at a number of frequencies and has been well-studied via polarimetric studies and timing analyses (see e.g. Stinebring et al. 1984; Shabanova 2010; Perera et al. 2015; Wahl et al. 2016).

* E-mail: golam.shaifullah@gmail.com

The timing study of Shabanova (2010) confirms a regular variation of the spin-down rate, $\dot{\nu} \equiv \Delta\nu/\Delta T$, where $\Delta\nu$ is the change in rotational frequency of the pulsar and ΔT is the time in days. They find that the spin-down rate variation has a ~ 600 d periodicity and follows a rough sawtooth-like behaviour. They also detect a glitch on MJD 55 140 (2009 November 5) leading to a fractional decrease in the spin period of $\delta P_0/P_0 \simeq 7.69 \times 10^{-5}$.

As mentioned earlier, PSR J0922+0638 also exhibits events marked by an aperiodic, rapid, and continuous decrease in the observed emission longitude (or pulse-phase) by up to 5° . These were first identified using observations from the Arecibo Observatory by Rankin et al. (2006a) at 327 and 1420 MHz, who called them ‘emission shifts’. The emission shifts were also identified in observations with the Jodrell Bank Observatory by Perera et al. (2015) who used pulsar timing analysis to measure variations in the spin-down rate of PSR J0922+0638. They find that the emission shifts (henceforth referred to as ‘events’ for brevity) of PSR J0922+0638 are not necessarily correlated with the two-state magnetospheric state switching cycle that PSR J0922+0638 experiences. However, they suggest similar events occurring with a much smaller phase variation could be related to the observed state switching. Using the Jiamusi 66-m telescope, Han et al. (2016) observed PSR J0922+0638 over ~ 30 h and were able to classify these events into four distinct morphologies. Wahl et al. (2016) searched for quasi-periodicities in these events using the data sets of Rankin et al. (2006a), complemented with new observations and archival data from the Arecibo Observatory as well as the observations of Han et al. (2016) and found no evidence for such periodicities in the case of PSR J0922+0638.

2 OBSERVATIONS

The observations presented in this article were carried out using the Effelsberg 100-m radio telescope and the Bornim (Potsdam) station of the LOw Frequency ARray (LOFAR; van Haarlem et al. 2013). At Effelsberg, the observations were carried out at 1350 MHz using the central beam of the 21-cm 7-beam receiver (Keller et al. 2006) and the PSRIX backend (Lazarus et al. 2016) which records coherently dedispersed observations for up to 300 MHz of bandwidth. Simultaneous observations using the 150-MHz high band antenna (HBA) tiles of the Bornim (Potsdam) LOFAR station (DE604) and the LOFAR und MPIfR Pulsare (LuMP) software¹ based backend were made possible by using the German Long Wavelength (GLOW)² mode. The observation details are presented in Table 1. For both the observing systems, data were coherently dedispersed and folded modulo the spin period to produce 10-s subintegrations and recorded with a final phase resolution of 0.35° per phase bin.

The observations were post-processed using the PSRCHIVE software suite³ (Hotan, van Straten & Manchester 2004; van Straten, Demorest & Osłowski 2012), radio frequency interference (RFI) was removed using the ‘median zapping’ option of the paz tool

Table 1. Details of observations carried out with the Bornim (Potsdam) LOFAR station and Effelsberg 100-m radio telescope in 2017 November.

Telescope	Effelsberg	DE604
Source name	J0922+0638	
Receiver name	P217-3	HBA
Name of the backend instrument	PSRIX	LuMP
Centre frequency (MHz)	1347.50	153.81
Weighted freq. (after RFI removal)	1352.98	152.12
Bandwidth (MHz)	200	71.48
Dispersion measure (pc cm ⁻³)	27.2951(6)	27.2951(6)
Number of pulse phase bins	1024	1024
Number of frequency channels	128	366
Polarizations recorded	Full Stokes	Full Stokes
Subintegration duration (s)	10.00	10.00
Number of subintegrations	703	703
Modified Julian Date	57705	57705

from PSRCHIVE followed by selective reweighting of strongly affected channels and subintegrations using a script from the COASTGUARD data processing pipeline (Lazarus et al. 2016). The timing solutions used in the ‘folding’ of the archives were corrected for spin-period offsets, measured using the TEMPO2 pulsar timing package (Hobbs, Edwards & Manchester 2006). The DM used for both the observations was measured from the LOFAR observations, by splitting them into four bands and fitting for the DM while the remaining timing parameters were held fixed. The data were polarization calibrated using the pac tool from PSRCHIVE. The method used for the Effelsberg utilizes standard, position offset observations with a calibrated noise diode while for the GLOW data, we use the method outlined in Noutsos et al. (2015).

3 DISCUSSION

Plots showing the intensity (colour-mapped to darker shades for higher values) as a function of the observing time and the rotational phase are presented in Fig. 1. On the left are the 1350 MHz Effelsberg observations while the 150 MHz LOFAR observations are plotted on the right.

Using the 1350 MHz observations to detect the events, we find a total of seven events, as shown in Fig. 1, five of which are easily visible and a further two which are only identified in the subintegration plots of Fig. 2. While it is not possible to recover the differing morphologies of these events as presented in the detailed single-pulse analysis by Han et al. (2016) we note that all seven events show differing degrees of pulse-phase variation and duration in our observations whose finest time resolution is limited to 10-s long subintegrations.

For each event, we also present subintegration plots in Fig. 2. The 1350 and 150 MHz plots have been scaled and smoothed independently. In spite of the scaling and smoothing, the low signal-to-noise ratio (S/N) due to excess RFI at the LOFAR bands often degrades the visibility of the integrated pulse profile. To facilitate comparison, Fig. 3 shows the integrated total intensity profile (black curve) for all the subintegrations which do not correspond to the events. The red and blue curves show the integrated linearly and circularly polarized intensities, respectively, while the top panel shows position angle (PA) measurements with a significance of 3σ or more for the same subintegrations. The dotted, grey curve shows the integrated total intensity profile for the event subintegrations, which have been plotted with thick black lines in Fig. 2.

¹<https://deki.mpifr-bonn.mpg.de/Cooperations/LOFAR/Software/LuMP>

²GLOW is the German Long-Wavelength consortium, an association of German universities and research institutes who share an interest in using the radio spectral window at metre wavelengths for astrophysical research. The International LOFAR stations in Germany, described in van Haarlem et al. (2013), are owned and run by GLOW member institutions and more details about the GLOW network are available here: <https://www.glowcohortium.de/index.php/en/>. We use the acronym to identify the operating mode, as well as the scheduling and monitoring software that allow the use of the GLOW stations for the observations presented here.

³<http://sourceforge.psrchive.org>

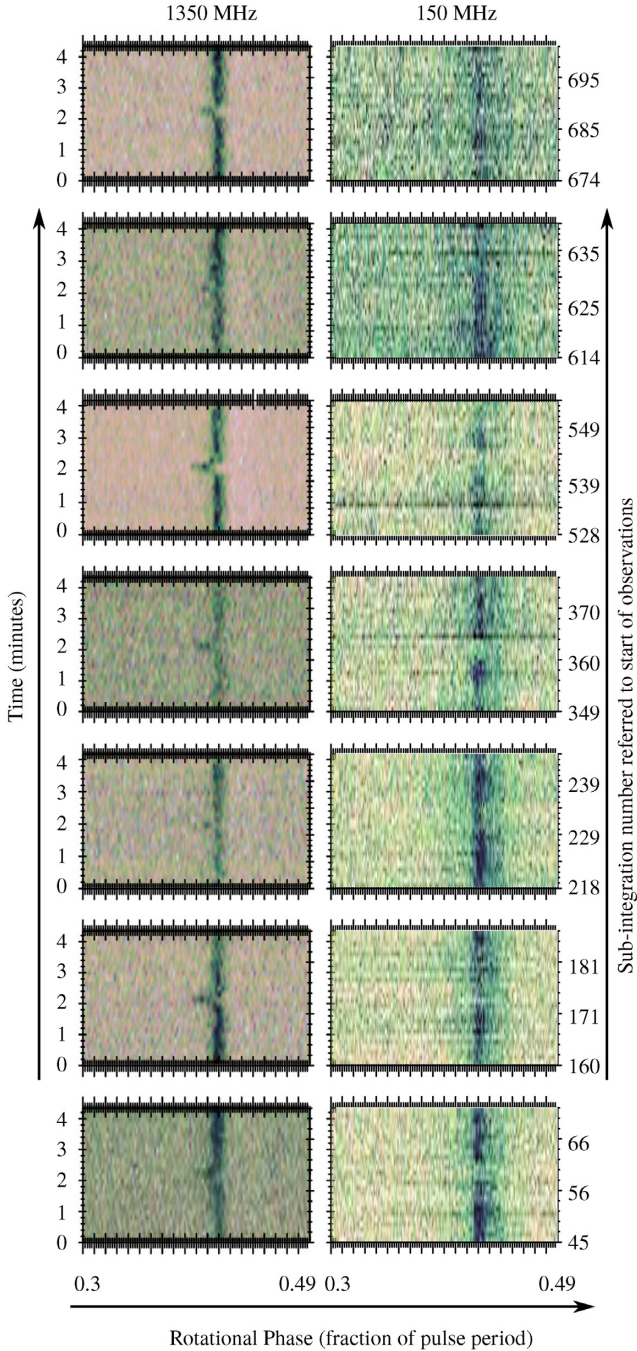


Figure 1. Observed intensity colour-mapped from lighter to darker shades plotted against the observation time (or subintegration number) and the rotational phase for the simultaneous observations from Effelsberg (left) and DE604 (right).

The majority of previous work on the emission shifts of PSR J0922+0638 were compiled using observations at 327, 1420, or 2400 MHz (see e.g. Rankin et al. 2006a; Perera et al. 2015; Han et al. 2016; Wahl et al. 2016) where these events are marked by a gradual shift of the emission phase to an earlier longitude without any change in the average flux density, as can be seen in the 1350 MHz observations in Fig. 1. However, at 150 MHz the events display a marked absence of emission at any shifted phase along with a significant decrease in the observed intensity at the usual

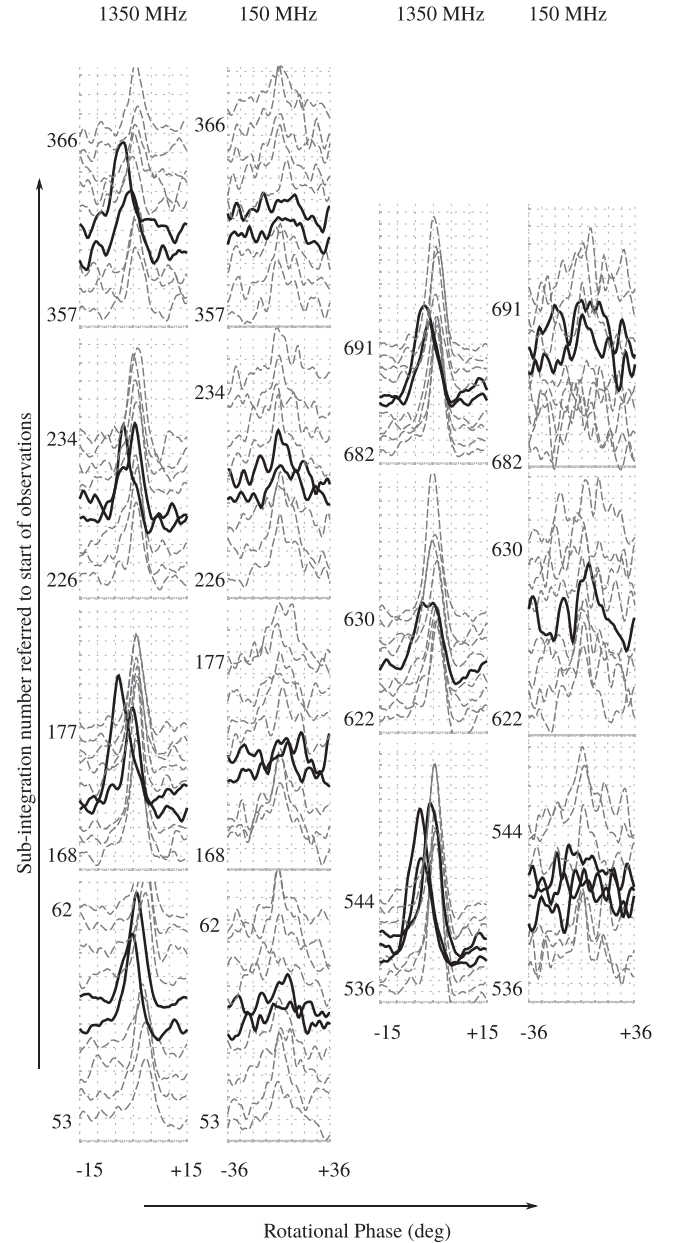


Figure 2. Subintegration plots of sections of the data presented in Fig. 1. Each curve shows the integrated flux for a 10-s subintegration. The amplitudes of the integrated pulse profiles have been scaled independently for the 1350 and 150 MHz data. The bold, solid lines show the ‘event’ subintegrations. Note the absence of a distinct profile for the corresponding regions of the 150 MHz plots.

phase. The integrated pulse profile for the events (dotted grey curve in Fig. 3) shows a significant but decreased amount of emission, although the profile shape is distorted due to the low S/N as only 14 subintegrations were combined to create the dotted grey profile compared to the remaining 689 for the solid black profile. Some of the observed power in the dotted grey profile is also due to the fact that the pulsar takes only a few to about 30 revolutions for the emission to diminish from or be restored to the typical observed flux density levels (see e.g. Rankin et al. 2006a; Han et al. 2016), which can occur on a time-scale much shorter than the 10-s subinte-

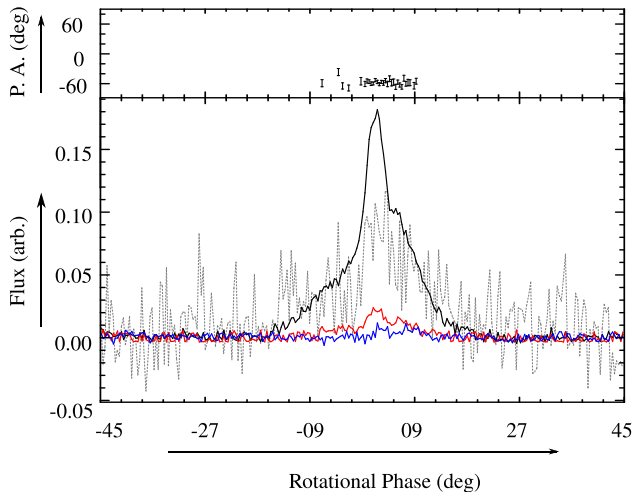


Figure 3. Integrated profile for the LOFAR observations with the ‘event’ subintegrations removed (solid black line) and only those subintegrations which are associated with an emission shift event added together separately (dotted grey line). The red and blue curves show the linearly and circularly polarized intensities, i.e. the $|L| \equiv |Q + iU|$ and $|V|$ Stokes components, respectively. The top panel shows the change in the position angle measured with a significance greater than 2σ .

grations in our data. As a result, a few of the subintegrations contain a fractional amount of power from the usual emission state.

In most cases the diminished emission at lower frequencies precedes and outlasts the emission shift at higher frequencies by a few subintegrations or tens of rotations. The change from ‘normal’ to diminished emission at the lower frequencies has a gradual onset and recovery, similar in the smoothness of its variation to the emission shift at higher frequencies although on distinctly longer time-scales. However, in keeping with its non-conformal behaviour, these diminished emission phases of PSR J0922+0638 show distinct variations amongst themselves as well. For example, in Fig. 2, for the coupled event at subintegrations 226–234, the decrease in emission lasts for less than a couple of subintegrations while for the event at subintegrations 357–366, the decrease precedes the shift by at least two subintegrations and does not recover to the normal profile for at least one subintegration after the shift has ended.

It is evident that the integrated data presented in our observations can only offer broad insights into this phenomenon and to gain a full description of the physical processes driving these changes, high S/N single-pulse data are necessary. However, even without the single-pulse data, it is possible to test some of the proposed origins of these events.

(i) ‘Absorption’ (Rankin et al. 2006a): The phenomenon of ‘absorption’ where the emission region is partly obscured has been one of the most promising candidates for explaining the complicated nature of the emission shifts of PSR J0922+0638. The archetypical example of this phenomenon is PSR J0814+7429 (B0809+74) (Rankin et al. 2006b) where part of the inherently broad profile is absorbed or occulted leading to distinct portions of the profile not being detected at certain frequencies.

We follow the approach presented in Rankin et al. (2006a), where this mechanism is first applied to explain these emission shifts and it is made clear that ‘absorption’ implies any physical process that might lead to part of the profile not being visible. However, in order to explain our observations this ‘absorption’ must also have a time dependent efficiency, along with the expected frequency

dependent behaviour. This is an added complexity over the case of PSR J0814+7429. There is a further constraint on the absorbing medium that it must always lead to an absorbed portion of profile at the leading edge at the LOFAR band while it must be more efficient at the regular emission phase only during the emission shift events at high frequencies. It is therefore abundantly clear that even if ‘absorption’ is the cause for the observed behaviour, the physical process leading to ‘absorption’ in this case might easily be very different from the typical examples.

(ii) Binary companions in light-cylinder orbits (Wahl et al. 2016): The absence of a true periodicity in the emission shifts of PSR J0922+0638 as well the extreme orbits and compositions necessary for such companions make such objects unlikely in the first place. Moreover, the necessity of similarity in the emission shifts at high and low frequencies is clearly in contrast to the observations.

(iii) Differentially corotating (entire) magnetosphere: Yuen & Melrose (2017) propose that the observed emission from a pulsar is due to the combination of the entire magnetosphere differentially corotating with respect to the stellar surface, structures around the magnetic pole (similar to the carousel model of Deshpande & Rankin 1999) and a moving visible emission region. They used seven components to model the observed profile of PSR J0922+0638, and this appears to predict the observed emission shift at 1400 MHz. As the components move due to variations in the magnetospheric rotation rate, this leads to different portions of the components crossing the line of sight, leading to the observed shift. While results for a lower frequency are not presented, the authors do point out that their approximations include ignoring a possible dependence of the magnetospheric plasma rotation rate on the radial distance from the centre of the pulsar. If such a dependence exists, it might be possible to explain the observed pseudo-nulling features at 100 MHz although this would still necessitate a very fortunate arrangement of the line of sight.

However, the change in the magnetospheric properties in the Yuen & Melrose (2017) model enters via their unphysical ‘y’ parameter. It is difficult to reconcile the variation of this global parameter with the absence of any correlation between the events and the magnetospheric state switching of PSR J0922+0638 observed by Perera et al. (2015).

(iv) Quasi-stable magnetosphere: There are hints that in some pulsars nulling and mode changing may be manifestations of the same phenomenon (see e.g. Wang, Manchester & Johnston 2007). It was suggested by Timokhin (2010) that magnetospheres can operate in different quasi-stable states with different sizes of the open field line zone or different current distributions in the radio emission region, or both. A magnetosphere can occasionally switch between these states and depending on our line of sight, we see either a different part of the emission cone, or we miss the entire cone resulting in the ‘null’ state. It was also shown that modest variations in the beam size can be accompanied by large variations in the pulsar spin-down rate. The combination of the effects of different current density distributions and different sizes of the emission cone could explain our observations of PSR J0922+0638, however as pointed out by Perera et al. (2015) there is no correlation between the events and the magnetospheric state switching.

(v) Frequency selective nulling: Using simultaneous multifrequency observations from 300 to 4850 MHz, Bhat et al. (2007) show that PSR J1136+1551 (B1133+16) shows ‘frequency selective’ nulling where nulls appear at one frequency even when emission is observed at another. The observations presented here might be explained by invoking frequency selective nulling only at the LOFAR bands, combined with either ‘absorption’ or apparent motion

of the line of sight with respect to the emission regions. However, it should be noted that in the case of PSR J1136+1551, the frequency selective nulling is not limited to the lowest frequencies only.

(vi) Intrinsic variations in the pulsar's beam combined with free-free absorption along the line of sight: Lewandowski et al. (2015) suggest that for the SGR J1745–2900 (also known as the Sgr A* magnetar or the Galactic Centre magnetar), expanding electronic ejecta due to outbursts can explain rapid variations in the observed radio spectrum of the magnetar. A similar mechanism in combination with intrinsic variations of the emission in the pulsar's beam would also be capable of explaining the observed phase shifting at higher frequencies and decreased emission in the LOFAR band.

4 CONCLUSIONS

In summary, simultaneous observations of PSR J0922+0638 using the Effelsberg 100-m radio telescope and the Bornim (Potsdam) LOFAR station demonstrate that during the previously identified phase shifts of the high-frequency emission, the emission at lower frequencies is strongly diminished, often appearing as null-like features accompanied by a marked absence of emission at any shifted phase. These null-like features strongly disfavour hypothetical binary companions. While models involving differential magnetospheric rotation rates could explain the observed variations, those models appear to be in tension with previous work which find no correlation between the switching of the magnetospheric states PSR J0922+0638 is believed to exhibit. It is possible that profile 'absorption' is indeed the mechanism due to which this emission shift is observed. However, the models of local 'absorption' in the emission region currently do not address the levels of complexity required to explain the time-varying yet distinct behaviour above and below ~250 MHz. These events might also arise due to a combination of intrinsic variations in the pulsar's beam with expanding screens of electrons along the line of sight.

However, a detailed analysis is beyond the scope of this letter and interested colleagues wishing to inspect the data presented here are encouraged to contact Jun. Prof. Verbiest or any of the leading authors for access to these and other, similar data sets.

ACKNOWLEDGEMENTS

The authors are grateful to the staff at the Effelsberg 100-m radio telescope and the GLOW consortium for their continued support for the respective telescopes which makes observations such as those presented here possible. GS acknowledges support from the Netherlands Organization for Scientific Research (NWO; TOP2.614.001.602), and is grateful to Gemma Janssen, Cees Bassa, and Yogesh Maan for useful discussions. SO acknowledges Australian Research Council grant Laureate Fellowship FL150100148. AS received funding from the NWO under project 'CleanMachine' (614.001.301). JK received funding from the German Federal Ministry of Education and Research (BMBF) under grant 05A14PBA (Verbundprojekt D-LOFAR III).

This paper is based (in part) on data obtained with LOFAR equipment. LOFAR (van Haarlem et al. 2013) is the LOW Frequency ARray, designed and constructed by ASTRON. We acknowledge the sup-

port and operation of the GLOW network, computing, and storage facilities by the Forschungszentrum Jülich, the Max-Planck-Institut für Radioastronomie, and Bielefeld University and financial support by the German states of Nordrhein-Westfalia and Hamburg.

REFERENCES

- Backer D. C., 1970a, *Nature*, 227, 692
 Backer D. C., 1970b, *Nature*, 228, 42
 Backer D. C., 1970c, *Nature*, 228, 1297
 Bhat N. D. R., Gupta Y., Kramer M., Karastergiou A., Lyne A. G., Johnston S., 2007, *A&A*, 462, 257
 Chatterjee S., Cordes J. M., Lazio T. J. W., Goss W. M., Fomalont E. B., Benson J. M., 2001, *ApJ*, 550, 287
 Cordes J. M., 1993, in Phillips J. A. Thorsett S. E. Kulkarni S. R., eds, ASP Conf. Ser. Vol. 36, Planets Around Pulsars. Astron. Soc. Pac., San Francisco, p. 43
 Deshpande A. A., Rankin J. M., 1999, *ApJ*, 524, 1008
 Gangadhara R., 1997, *A&A*, 327, 155
 Han J. et al., 2016, *MNRAS*, 456, 3413
 Hobbs G. B., Edwards R. T., Manchester R. N., 2006, *MNRAS*, 369, 655
 Hotan A. W., van Straten W., Manchester R. N., 2004, *PASA*, 21, 302
 Johnston S., van Straten W., Kramer M., Bailes M., 2001, *ApJ*, 549, L101
 Johnston S., Hobbs G., Vigeland S., Kramer M., Weisberg J. M., Lyne A. G., 2005, *MNRAS*, 364, 1397
 Keller R. et al., 2006, Technical report, Multi-Beam Receiver for Beam-Park Experiments and Data Collection Unit for Beam Park Experiments with Multi-Beam Receivers. Max Planck Institut für Radioastronomie
 Lazarus P., Karuppusamy R., Graikou E., Caballero R. N., Champion D. J., Lee K. J., Verbiest J. P. W., Kramer M., 2016, *MNRAS*, 458, 868
 Lewandowski W., Rożko K., Kijak J., Melikidze G. I., 2015, *ApJ*, 808, 18
 McKee J. W. et al., 2016, *MNRAS*, 461, 2809
 Noutsos A. et al., 2015, *A&A*, 576, A62
 Osłowski S., van Straten W., Hobbs G. B., Bailes M., Demorest P., 2011, *MNRAS*, 418, 1258
 Perera B. B. P., Stappers B. W., Weltevrede P., Lyne A. G., Bassa C. G., 2015, *MNRAS*, 446, 1380
 Petit G., Tavella P., 1996, *A&A*, 308, 290
 Radhakrishnan V., Manchester R. N., 1969, *Nature*, 222, 228
 Rankin J. M., Rodriguez C., Wright G. A. E., 2006a, *MNRAS*, 370, 673
 Rankin J. M., Ramachandran R., Suleymanova S. A., 2006b, *A&A*, 447, 235
 Reichley P. E., Downs G. S., 1969, *Nature*, 222, 229
 Shabanova T. V., 2010, *ApJ*, 721, 251
 Stinebring D. R., Cordes J. M., Rankin J. M., Weisberg J. M., Boriakoff V., 1984, *ApJS*, 55, 247
 Stovall K. et al., 2015, *ApJ*, 808, 156
 Timokhin A. N., 2010, *MNRAS*, 408, L41
 van Haarlem M. P. et al., 2013, *A&A*, 556, A2
 van Straten W., Tiburzi C., 2017, *ApJ*, 835, 293
 van Straten W., Demorest P., Osłowski S., 2012, *Astron. Res. Technol.*, 9, 237
 Verbiest J. P. W. et al., 2009, *MNRAS*, 400, 951
 Wahl H. M., Orfeo D. J., Rankin J. M., Weisberg J. M., 2016, *MNRAS*, 461, 3740
 Wang N., Manchester R. N., Johnston S., 2007, *MNRAS*, 377, 1383
 Yuen R., Melrose D. B., 2017, *MNRAS*, 469, 2049

This paper has been typeset from a $\text{\TeX}/\text{\LaTeX}$ file prepared by the author.